



Volume 1 Issue 2

Transparent Sheet Heater With Flexibility Based on Poly (Vinyl Alcohol) Embedded With Sodium Tungstate

Deepa Joshi^a, Aboobakar Savanur^a, Laxmibai P. Rathod^a, Sridhar N. Mathad^b, Arun Y. Patil^c, and Mallikarjunagouda B. Patil^{*a}

^aBharat Ratna Prof. CNR Rao Research Centre, Basaveshwar Science College, Bagalkot, Karnataka, India 587101

^bDepartment of Engineering Physics, KLE Institute of Technology, Hubballai, Karnataka, India 580027

^cSchool of Mechanical Engineering, KLE Technological University, Vidya Nagar, Hubballi, India 580031

Abstract

Transparent sheet heaters with flexibility (TSHF) exhibiting improved mechanical and thermal stability were made by adding sodium tungstate (NaW) into poly (vinyl alcohol) (PVA) films by solution coating and solvent evaporation method. The prepared TSHFs were characterized by scanning electron microscopy (SEM) to understand the surface morphology better. Further UV-Visible measurement was carried out. The electric conductive properties were assessed by using the four-probe experiment. An infrared thermometer was used to measure the temperature of the TSHFs. The fabricated NaW/PVA hybrid TSHFs demonstrated elevated heating temperatures, 96 °C at a minimum input voltage of 6 V with a minimum response time ($T < 40$ sec), lower power consumption ($162 \text{ }^\circ\text{C cm}^2 \text{ W}^{-1}$) and process stability after repeated use when compared to ITO/FTO heaters. The bending resistance of the NaW/PVA hybrid TSHFs was excellent. The change in sheet resistance after 1000 cycles of outer bending was less than 18%. The effective embedding of the NaW network in the transparent nascent PVA film's surface reduced surface roughness ($R_{\text{rms}} < 1$ nm) and improved oxidation and moisture resistance. The produced TSHFs exhibited excellent heating qualities, with their transparency demonstrating remarkable flexibility. The potential uses of NaW/PVA include defogging windows and thermochromic.

Keywords: Transparent Thin-Film Heaters; Flexible Transparent Electrodes; Conductive Films; Poly(Vinyl Alcohol); Sodium Tungstate

1 Introduction

Transparent film heaters (TFHs) have received much attention for a variety of applications, including outdoor displays, window defogging, and thermal-based sensors [1–5]. A typical commercial film-like heater is made of a metallic wire based on a Fe-Cr-Al alloy [6], which, however, is rigid and has a low heating efficiency. Another commercial metallic film heater with similar shortcomings is a patterned copper foil thin film [7]. Tin-doped indium oxide (ITO) transparent conductive film has also been widely used as a heating element because of its high optical transmittance in the visible region, high electrical conductivity, and environmental stability [8–10]. However, due to indium scarcity, crack formation during mechanical bending, and delayed thermal response, ITO is considered prohibitively expensive, particularly in large areas and flexible applications [11–15]. Several electrically conductive materials, such as carbon nanotubes, graphene [16–19] and metal grids [20–23], have been investigated as potential replacements for ITO.

*Corresponding author: mallupatil04@gmail.com

Received: 19 September 2022; Accepted: 02 December 2022; Published: 31 December 2022

© 2022 Journal of Computers, Mechanical and Management.

This is an open access article and is licensed under a [Creative Commons Attribution-Non Commercial 4.0 International License](https://creativecommons.org/licenses/by-nc/4.0/).

DOI: [10.57159/gadl.jcmm.1.2.23016](https://doi.org/10.57159/gadl.jcmm.1.2.23016).

When used as flexible TFHs, such materials promise to provide uniform thermal distribution over the heating area and reach higher temperatures at low power [24]. Silver nanowires (AgNWs) have emerged as interesting candidates for the fabrication of TFHs because of their good conductivity, high transparency, and appropriate mechanical qualities [25–27], and there have been reports of TFHs based on AgNWs [28–30]. The reported TFHs were created by depositing AgNWs on the surface of a transparent polymer substrate, such as polyethylene naphthalate (PEN) or polyethylene terephthalate (PET), and as they have low thermal resistance, the fabricated AgNW-based film heaters could only attain a certain temperature. Furthermore, the adhesion between the AgNWs and the substrate was weak, and the AgNW network on these substrates was scratch-resistant and easily detached, resulting in low conductivity and inefficient heat production. Thus, filling the gap in the existing literature, the present study describes the in-situ fabrication of transparent sheet heaters with flexibility (TSHF) comprised of a NaW network embedded in a transparent poly(vinyl alcohol) (PVA) film. The NaW/PVA TSHFs are designed to have a desirable combination of properties such as high glass transition temperature (T_g), mechanical flexibility, visual transparency and a strong bonding force with NaW. The TSHFs made from this composite exhibited a high saturation temperature attainment of up to 96 °C, could be heated quickly at lower operation voltages and had only a slight temperature variation over a long period of heating at a constant voltage.

2 Materials and Method

All reagents used in this study were obtained from E. Merck and included poly(vinyl alcohol) (PVA), sodium tungstate (NaW), acetone, and ethanol. Tetraethoxysilane (TEOS ;98%) was purchased from Sigma-Aldrich. All reagents and chemicals used were of analytical grade. Under vigorous stirring, 5 g of PVA was dissolved in 80 ml distilled water. For 6 hrs, the temperature was maintained constant at 70 °C. After preparing a homogeneous transparent solution, 0.5 gm of tetra ethyl orthosilicate (TEOS) was added, followed by 3-4 drops of HCl as a catalyst. The solution was stirred and maintained at 70°C for another 6 hrs, and then, after the completion of the reaction, the solution was allowed to cool. A gravimetric ratio of sodium tungstate was added to the mixture and stirred for 1 hr. After pouring the slurry mentioned above onto the thick transparent sheet, as shown in Figure 1, a 5 mm Finolex make pure copper wire was inserted into the cast at a distance of 10 cm from both edges of the film. The dimensions of the film were 10 X 5 cm. Two wires from each copper stripe were connected when the copper wires were stretched beyond the sample length, as illustrated in Figure 1.

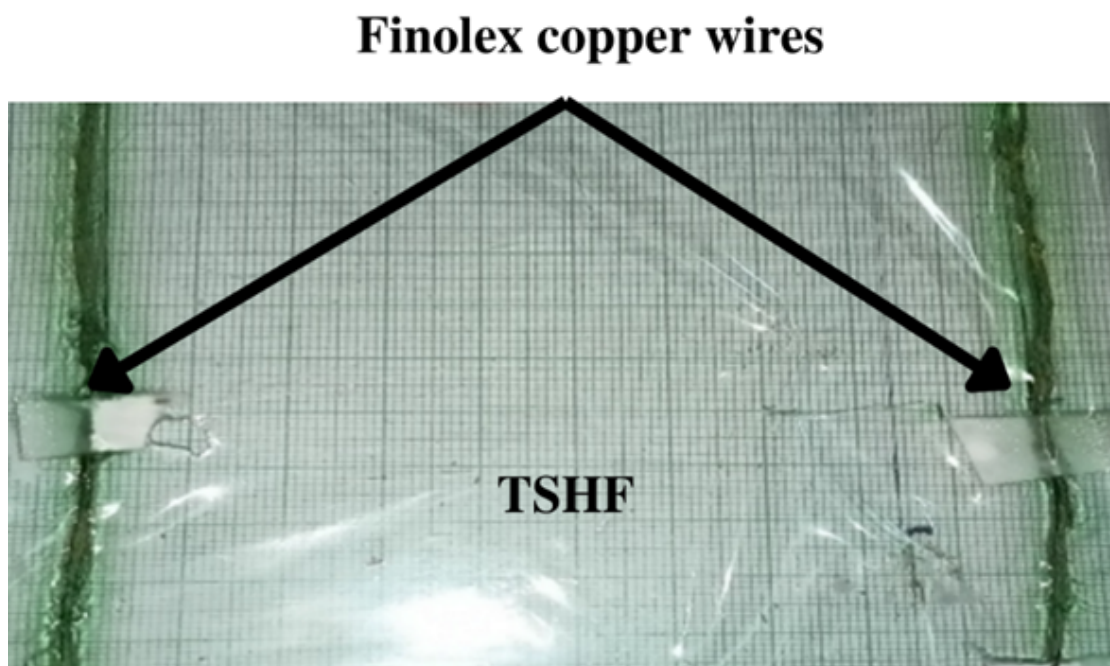


Figure 1: Copper wires attached to the transparent sheet

The concentration and nomenclature of the prepared NaW and PVA films are shown in Table 1. The surface morphologies of NaW/PVA TSHFs were analyzed using scanning electron microscopy (SEM), wherein the SEM images were taken after sputter coating the specimen with gold. The optical transmittance of the transparent PVA film and NaW/PVA TSHFs was measured at room temperature using an ultraviolet-visible spectrophotometer with an integrating sphere, and the sheet resistance of NaW/PVA TSHFs was measured using a four-point probe system. A power source supplied DC voltage to the TSHFs through the copper contact attached at the edge of the film. The temperature of the TSHFs was measured with an infrared thermometer. To accurately reflect the thermal distribution, nine temperature points were measured for each TSHF, and the average value was recorded. Mechanical stability tests were performed using a laboratory-installed bending test machine. The moisture test was carried out using a highly accelerated temperature and humidity stress test (HAST) at a temperature of 120 °C, a relative humidity (RH) of 97% and a gauge pressure of 0.1 MPa. The adhesion test was performed using 3M stock tape.

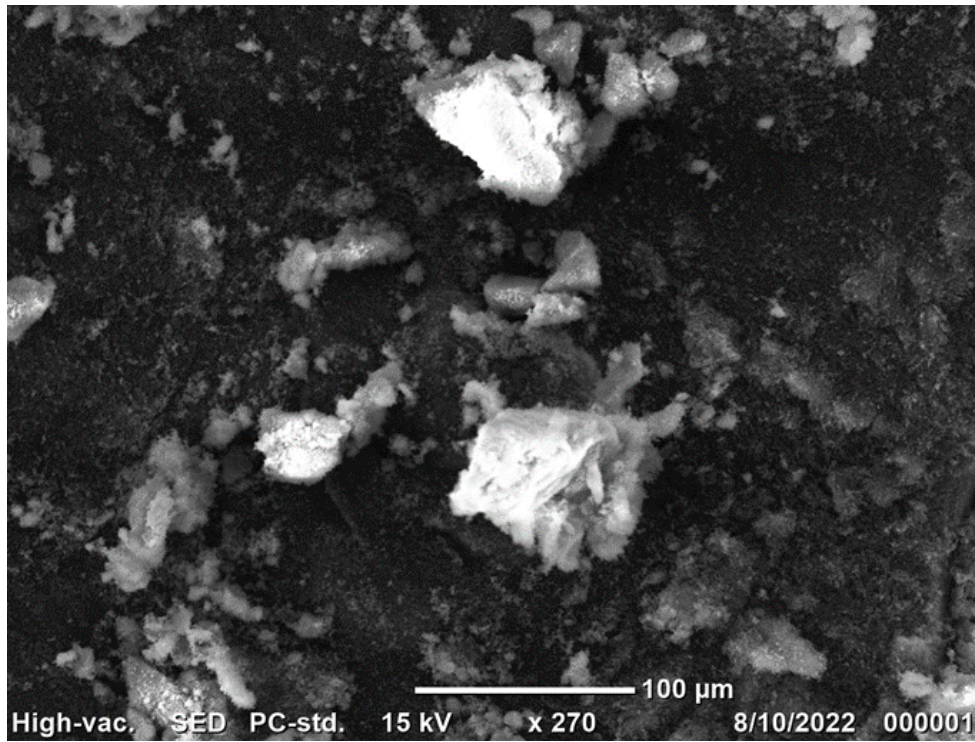


Figure 2: SEM image of the prepared NaW/PVA transparent sheet heater with flexibility.

Table 1: Concentration and nomenclature of the prepared heater films

Sl. No	PVA (g)	Sodium Molybdate (g)	Sodium Molybdate (%)	Film Name
1	5	0.000	0.0	Plain PVA
2	5	0.125	2.5	2.5-NaW/PVA
3	5	0.250	5.0	5-NaW/PVA
4	5	0.375	7.5	7.5-NaW/PVA
5	5	0.500	10.0	10-NaW/PVA

3 Results and Discussion

3.1 Surface morphologies of the prepared NaW/PVA TSHFs

Figure 2 depicts the SEM image of the prepared NaW/PVA TSHF, which exhibits a smooth surface and a well-connected point-to-point junction. The NaW molecules are inlaid on the surface of the films. There were no voids on the surface. Thus, it indicates that all NaW has been transferred to the surface of the PVA film. The surface morphology indicates that the transparent PVA solution thoroughly permeated the NaW network and filled network holes and voids at the interface of the NaW and the rigid substrate.

3.2 Optical and electrical properties of the prepared NaW/PVA TSHFs

Fig 3 depicts the optical transmittance spectra of the TSHFs with increasing refractive index (N). Each TSHF's sheet resistance values are also provided. At 550 nm, the pure PVA film demonstrated a high optical transmittance of 92%. The transmittance of TSHFs decreased as the number of N increased after the NaWs were inserted. The light reflection and scattering from the NaWs caused this change. Furthermore, as N increased, the sheet resistance of the TSHFs decreased. The sheet resistance of the 3NaW/PVA (N=3) sample was 10×10^{-3} Ohm/sq with a transmittance of 83% at 550 nm, whereas the sheet resistance of the 12AgNW/PI (N = 12) sample was 5.6 Ohm/sq with a transmittance of 58% at 550 nm. The findings suggested that the NaW density could be tweaked to improve the optical and electrical properties of NaW/PVA TSHFs.

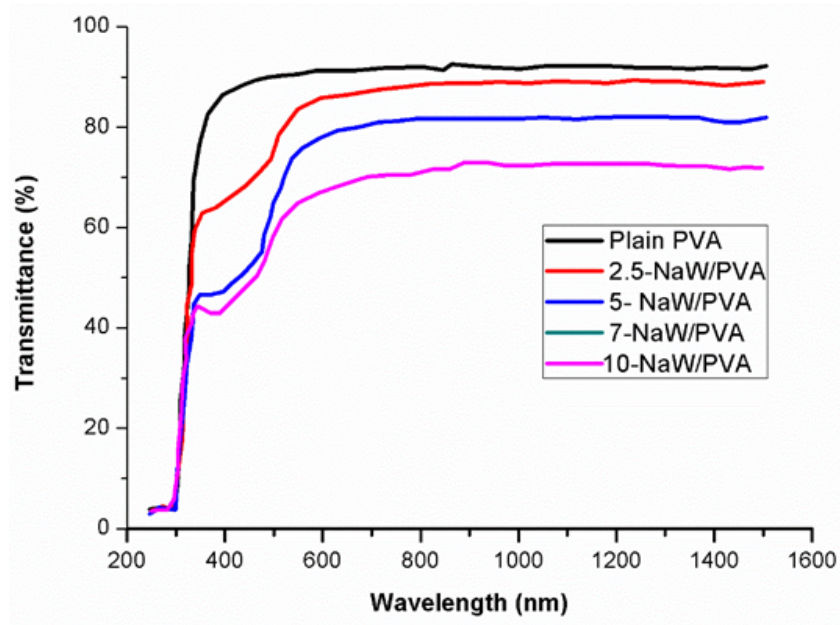


Figure 3: Optical transmittance spectra of the plain PVA film, TSHFs, and the sheet resistance of TSHFs.

3.3 Thermal response behavior of the prepared NaW/PVA TSHFs

The temperature properties of NaW/PVA TSHFs were investigated to better understand the nature of Joule heating in TSHFs. Figure 4 depicts the recorded temperature measurements graphically. The NaW/PVA TSHFs used in this section were 2.5 cm × 2.5 cm in size. Figure 4 depicts the temperature profiles of the TSHFs as a function of input voltage (modulated from 1 to 6 V). The TSHFs used had an optoelectronic performance of 5.6 Ohm/sq and a transmittance of 58% at 550 nm. When the input voltage was set to 1 V, all the plots showed that the temperature of the TSHFs reached 30 °C. The temperature of the TSHFs reached above 96 °C when the input voltage was increased to 6 V, confirming its good operation at a low input voltage. Higher power at a low input voltage implies efficient electrical energy conversion to Joule heating. One of the key factors for evaluating the performance of TSHFs is the response time, which is defined as the time required to reach the steady-state temperature ($T_{\text{steady-state}}$) from room temperature (T_{room}). Regardless of the applied voltage, the temperature increased quickly, and steady-state temperatures were reached in less than 40 sec, demonstrating the device’s quick response. Power consumption, defined as temperature increase per unit of electrical power input, is another important parameter for assessing heat performance, which was investigated in the present work by applying Joule’s law to the heat generated by a film heater using Eq. [1].

$$P = \frac{U^2}{R} \quad (1)$$

where P is the applied voltage, U is the input power, and R is the resistance of the film heater to which the voltage is applied. Figure 4 indicates the input power of the NaW/PVA TSHFs as a function of steady-state temperature and the input power as a function of steady-state temperature. Based on the data analyzed and the size of the TSHFs, the electrical power consumption of the TSHFs was calculated and found to be around 162 °C cm²W⁻¹.

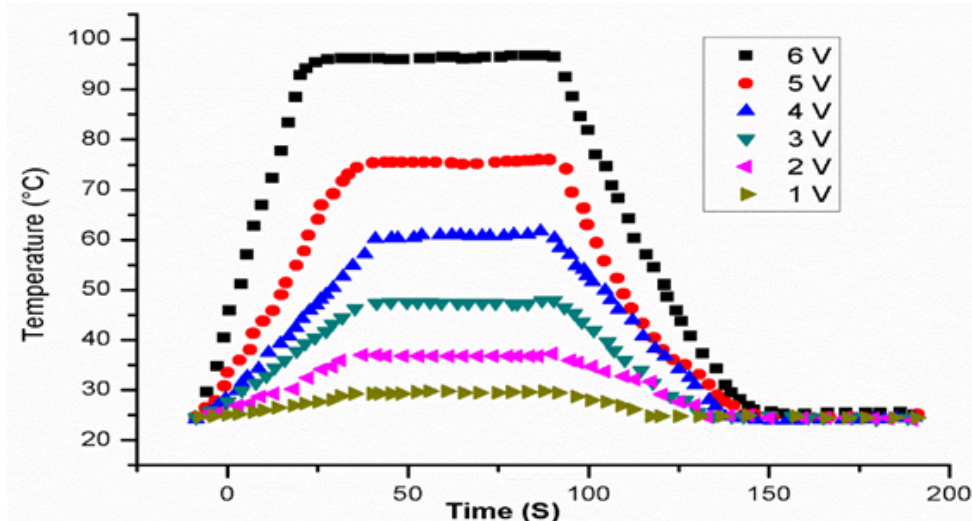


Figure 4: Temperature profiles of NaW/PVA TSHFs as a function of input voltage.

It was observed further that the temperature-time curves remained unchanged while the maximum temperature increased slightly, as seen in Figure 5. Stability tests at an applied bias for 1 hour revealed no significant degradation in achievable temperature, demonstrating the stability for repeated and long-term use. The slight increase in maximum temperature shown in Figure 5 suggested that a slight decrease in heater resistance could be attributed to more tightly connected nanowires. To investigate the thermal response of the NaW/PVA TSHFs that were created, the relationship between the $T_{\text{steady-state}}$ and T_{room} of the NaW/PVA TSHFs is expressed using Eq.[2].

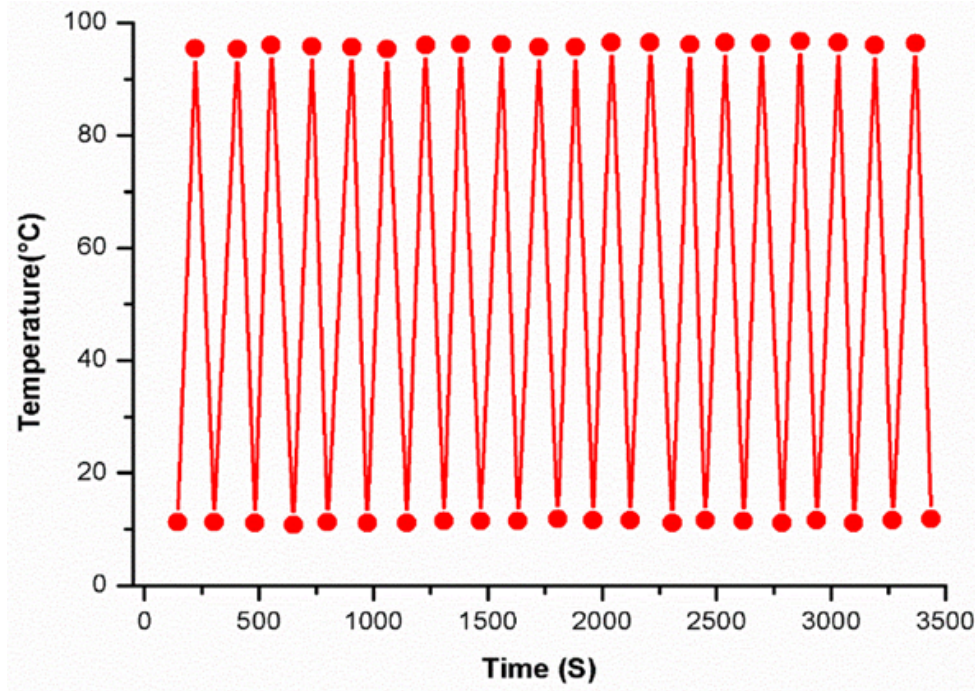


Figure 5: Cycling performance of AgNW/PVA TSHF with a sheet resistance of 5.6 Ohm/sq.

$$T_{\text{steady-state}} = \left(\frac{U^2}{R} - Q_d \right) \frac{1}{C_m} + T_{\text{room}} \quad (2)$$

where C is the heat capacity ratio of the film, m is the film mass, and Q_d is the heat dissipated from the film. Heat dissipation is the transfer of heat by radiation and convection. At temperatures below 150 °C, radiation was found to be negligible. The significant path of heat dissipation was through air convection, and $T_{\text{steady-state}}$ could be attained when Joule heating and convection reach a dynamic balance at elevated temperatures. When the sample geometry is fixed, Eq. (2) shows that $T_{\text{steady-state}}$ increases with increasing voltage U and decreases with decreasing resistance R , or the sheet resistance of the film heater. The maximum temperature at steady state increased as the sheet resistance of the NaW/PVA TSHFs decreased under the same input voltage (6 V), implying that the sheet resistance value of the film should be less than 60 Ohm sq^{-1} to allow for a maximum temperature above 72 °C.

3.4 Mechanical behavior of the prepared NaW/PVA TSHFs

Aside from having excellent surface morphology and thermal response behavior, the prepared NaW/PVA TSHFs exhibited superior mechanical flexibility, which is desirable for emerging flexible electronic devices. Outer and inner bending tests were carried out on a lab-installed bending test system with a fixed bending radius of 5 mm that was controlled as a function of the number of bending cycles. The nominal bending strain was determined using Eq.[3].

$$\epsilon_f = \frac{h}{2r} \quad (3)$$

Figure 6 depicts the change in sheet resistance in the prepared TSHFs. $R = \frac{(R-R_0)}{R_0}$ represents the change in film resistance, where R_0 is the initial sheet resistance and R is the value measured after the bending test. The resistance changes were recorded three times for each bending cycle to ensure measurement accuracy. The resistance changes in the outer and inner bending tests were determined as 0.17% and 0.312%, respectively. Because of the strong bonding between the transparent PVA film and the NaWs network, the electrical properties of the prepared TSHFs were more resistant to outer and inner bending. Under extreme bending, such a strong bond prevents sliding at the interface. Furthermore, a change in the sheet resistance of the prepared TSHFs under extreme folding and crumpling conditions was also observed.

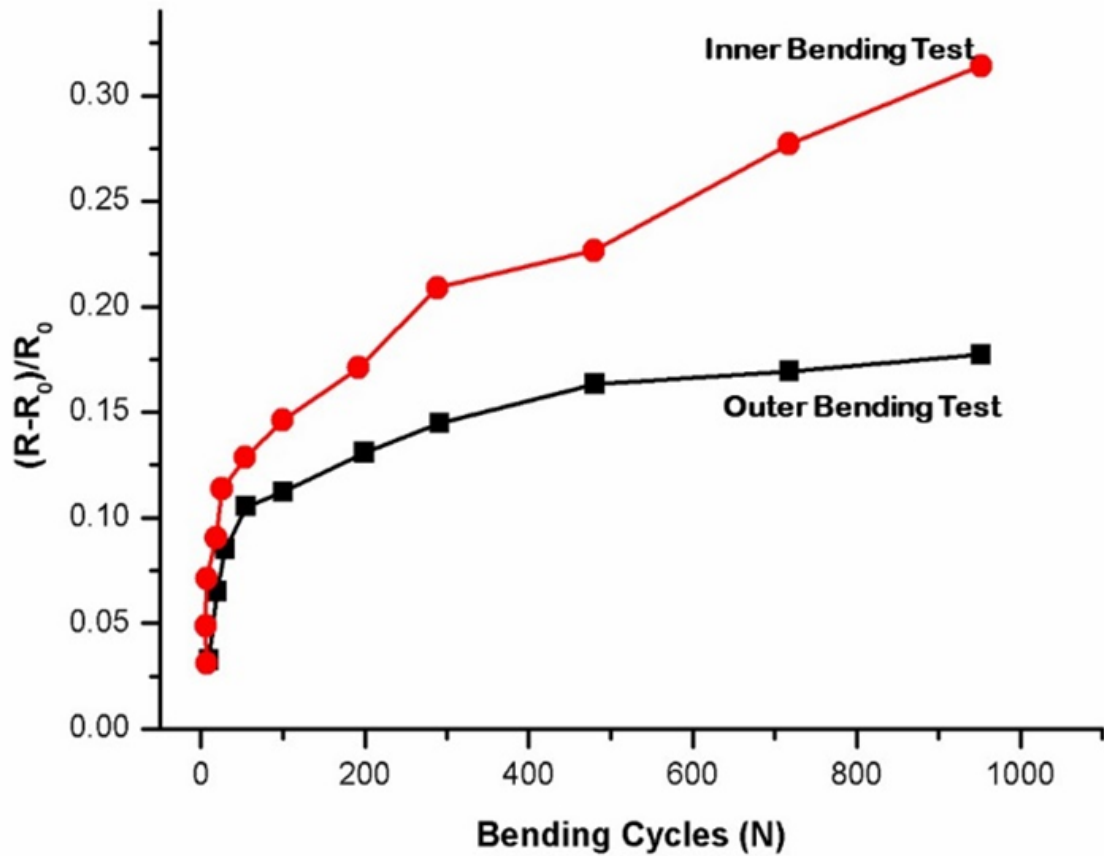


Figure 6: Sheet resistance change of the NaW/PVA TSFHs.

3.5 Moisture behavior of the prepared NaW/PVA TSFHs

The optical and electrical performances of prepared TSFHs were evaluated in a humidity chamber (122 °C, 97% relative humidity for 24 hrs) for thermal moisture testing to confirm long-term reliability. The optical and electrical properties of the prepared TSFHs before and after thermal moisture testing are shown in Figure 7(a). The change in the PVA film in the harsh environment caused a slight decrease in transmittance (T_{550} , before = 64.0% and T_{550} , after = 61.0%). The resistance increase was primarily caused by the oxidation of a small amount of NaWs exposed on the surface of the prepared NaW/PVA TSFHs. The thermal response of the NaW/PVA TSFHs before and after thermal moisture testing is depicted in Figure 7(b). $T_{\text{steady-state}}$ dropped from 76 °C to 74 °C. Because of the nearly stable heating temperature, the prepared TSFHs can be used in defrosting window panels applications in outdoor advertisement boards. The TSFHs' adhesion was tested by repeatedly sticking and peeling them. On the surface of the TSFHs, 3M Scotch tape was applied. The sheet resistance increased by only 0.057 after 1000 adhesion peeling cycles, indicating a strong bonding of the conductive nanowires on the TSFHs.

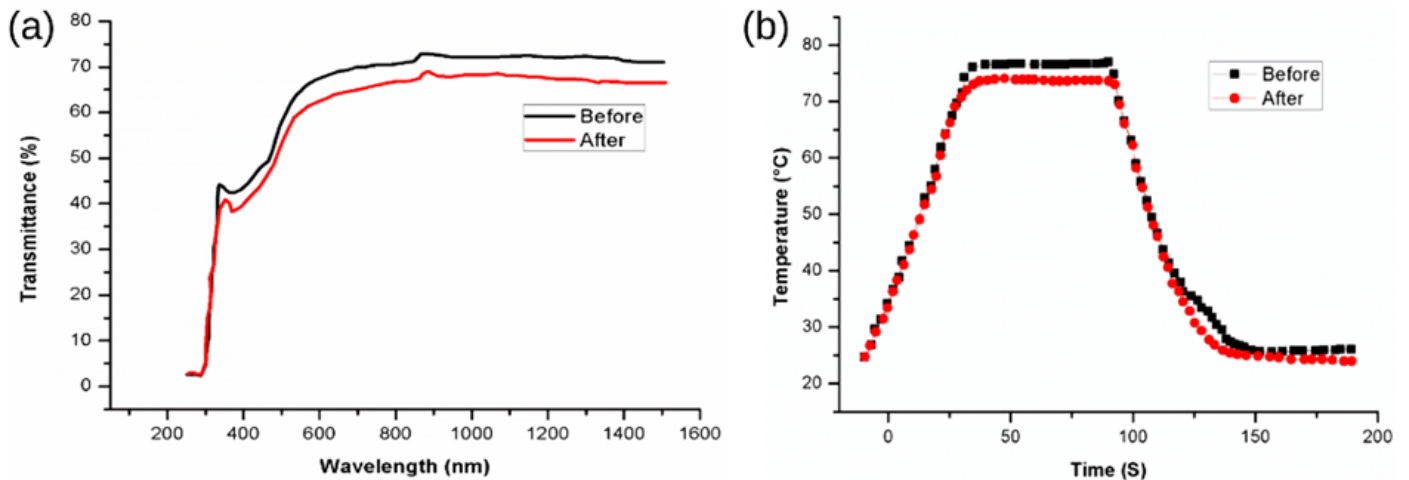


Figure 7: (a) Optical and electrical properties of the prepared TSFHs before and after thermal moisture testing, and (b) Thermal response of the NaW/PVA TSFHs before and after thermal moisture testing.

4 Conclusion

A solution process was used to create flexible TSFHs with a NaWs network embedded in the surface of a transparent PVA film. A typical NaW/PVA TSFH with a low sheet resistance of 5.6 Ohm/sq and a transmittance of 58.0% were obtained by adjusting the number of rod-coating cycles of the NaW suspension. Thermal response tests on NaW/PVA TSFHs revealed a higher heating temperature of 97 °C, a fast response time of less than 40 sec, and lower power consumption of 161.2 °C cm²W⁻¹, as well as repeatability. NaW/PVA TSFH mechanical properties were also investigated. The resistance changes in the outer and inner bending tests were 0.18% and 0.31%, respectively. Furthermore, after 24 hours of testing in a humidity chamber at 122 °C/97% relative humidity, the NaW/PVA TSFHs demonstrated nearly stable optical properties, sheet resistance, and heating temperatures. As a result, the fabricated NaW/PVA TSFHs may find use in window defogging, thermochromic, and transparent electrodes.

Declaration of Competing Interests

The author declares that she has no known competing financial interests or personal relationships that could have appeared to influence the work reported in this paper.

Funding Declaration

This work was supported by the Vision Group for Science and Technology (VGST), Govt. of Karnataka, Bengaluru, India, under grant number GRD No: 951 (2020–2021) for establishing the laboratory at Basaveshwar Science College, Bagalkot, India.

Author Contribution

Deepa Joshi: Conceptualization, Methodology; **Aboobakar Savanur:** Data curation, Writing- Original draft preparation; **Laxmibai Rathod:** Visualization, Investigation; **Mallikarjunagouda Patil:** Supervision, Reviewing and Editing, Validation; **Arun Y Patil:** Writing- Reviewing; **S N Mathad:** Writing- Reviewing.

References

- [1] Y. H. Yoon, J. W. Song, D. Kim, J. Kim, J. K. Park, S. K. Oh, and C. S. Han, "Transparent film heater using single-walled carbon nanotubes," *Advanced Materials*, vol. 19, no. 23, pp. 4284–4287, 2007.
- [2] X. Y. Zeng, Q. K. Zhang, R. M. Yu, and C. Z. Lu, "A new transparent conductor: Silver nanowire film buried at the surface of a transparent polymer," *Advanced Materials*, vol. 22, no. 40, pp. 4484–4488, 2010.
- [3] D. Jung, D. Kim, K. H. Lee, L. J. Overzet, and G. S. Lee, "Transparent film heaters using multi-walled carbon nanotube sheets," *Sensors and Actuators, A: Physical*, vol. 199, pp. 176–180, 2013.
- [4] B. Han, Y. Huang, R. Li, Q. Peng, J. Luo, K. Pei, A. Herczynski, K. Kempa, Z. Ren, and J. Gao, "Bio-inspired networks for optoelectronic applications," *Nature Communications*, vol. 5, no. 1, p. 5674, 2014.
- [5] J. Song and H. Zeng, "Transparent electrodes printed with nanocrystal inks for flexible smart devices," *Angewandte Chemie - International Edition*, vol. 54, no. 34, pp. 9760–9774, 2015.
- [6] Z. P. Wu and J. N. Wang, "Preparation of large-area double-walled carbon nanotube films and application as film heater," *Physica E: Low-Dimensional Systems and Nanostructures*, vol. 42, no. 1, pp. 77–81, 2009.
- [7] Y. A. Li, Y. J. Chen, and N. H. Tai, "Highly thermal conductivity and infrared emissivity of flexible transparent film heaters utilizing silver decorated carbon nanomaterials as fillers," *Materials Research Express*, vol. 1, no. 2, p. 025605, 2014.
- [8] R. G. Gordon, "Criteria for choosing transparent conductors," *MRS Bulletin*, vol. 25, no. 8, pp. 52–57, 2000.
- [9] K. Im, K. Cho, J. Kim, and S. Kim, "Transparent heaters based on solution-processed indium tin oxide nanoparticles," *Thin Solid Films*, vol. 518, no. 14, pp. 3960–3963, 2010.
- [10] A. Y. Kim, K. Lee, J. H. Park, D. Byun, and J. K. Lee, "Double-layer effect on electrothermal properties of transparent heaters," *Physica Status Solidi (A) Applications and Materials Science*, vol. 211, no. 8, pp. 1923–1927, 2014.
- [11] P. C. Hsu, S. Wang, H. Wu, V. K. Narasimhan, D. Kong, H. R. Lee, and Y. Cui, "Performance enhancement of metal nanowire transparent conducting electrodes by mesoscale metal wires," *Nature Communications*, vol. 4, no. 1, p. 2522, 2013.

- [12] B. Han, K. Pei, Y. Huang, X. Zhang, Q. Rong, Q. Lin, Y. Guo, T. Sun, C. Guo, D. Carnahan, M. Giersig, Y. Wang, J. Gao, Z. Ren, and K. Kempa, "Uniform self-forming metallic network as a high-performance transparent conductive electrode," *Advanced Materials*, vol. 26, no. 6, pp. 873–877, 2014.
- [13] Q. Xu, W. Shen, Q. Huang, Y. Yang, R. Tan, K. Zhu, N. Dai, and W. Song, "Flexible transparent conductive films on PET substrates with an AZO/AgNW/AZO sandwich structure," *Journal of Materials Chemistry C*, vol. 2, no. 19, pp. 3750–3755, 2014.
- [14] C. Zhu, J. Li, Y. Yang, J. Huang, Y. Lu, R. Tan, N. Dai, and W. Song, "Zn-aided defect control for ultrathin GZO films with high carrier concentration aiming at alternative plasmonic metamaterials," *Physica Status Solidi (A) Applications and Materials Science*, vol. 212, no. 8, pp. 1713–1718, 2015.
- [15] J. Song, S. A. Kulinich, J. Li, Y. Liu, and H. Zeng, "A general one-pot strategy for the synthesis of high-performance transparent-conducting-oxide nanocrystal inks for all-solution-processed devices," *Angewandte Chemie - International Edition*, vol. 54, no. 2, pp. 462–466, 2015.
- [16] J. S. Woo, J. T. Han, S. Jung, J. I. Jang, H. Y. Kim, H. J. Jeong, S. Y. Jeong, K. J. Baeg, and G. W. Lee, "Electrically robust metal nanowire network formation by in-situ interconnection with single-walled carbon nanotubes," *Scientific Reports*, vol. 4, no. 1, p. 4804, 2014.
- [17] J. Kang, H. Kim, K. S. Kim, S. K. Lee, S. Bae, J. H. Ahn, Y. J. Kim, J. B. Choi, and B. H. Hong, "High-performance graphene-based transparent flexible heaters," *Nano Letters*, vol. 11, no. 12, pp. 5154–5158, 2011.
- [18] J. Wang, Z. Fang, H. Zhu, B. Gao, S. Garner, P. Cimo, Z. Barcikowski, A. Mignerey, and L. Hu, "Flexible, transparent, and conductive defrosting glass," *Thin Solid Films*, vol. 556, pp. 13–17, 2014.
- [19] X. Zhang, X. Yan, J. Chen, and J. Zhao, "Large-size graphene microsheets as a protective layer for transparent conductive silver nanowire film heaters," *Carbon*, vol. 69, pp. 437–443, 2014.
- [20] N. Kwon, K. Kim, J. Heo, I. Yi, and I. Chung, "Study on Ag mesh/conductive oxide hybrid transparent electrode for film heaters," *Nanotechnology*, vol. 25, no. 26, p. 265702, 2014.
- [21] K. D. M. Rao and G. U. Kulkarni, "A highly crystalline single Au wire network as a high temperature transparent heater," *Nanoscale*, vol. 6, no. 11, pp. 5645–5651, 2014.
- [22] S. Kiruthika, R. Gupta, and G. U. Kulkarni, "Large area defrosting windows based on electrothermal heating of highly conducting and transmitting Ag wire mesh," *RSC Advances*, vol. 4, no. 91, pp. 49745–49751, 2014.
- [23] J. Song, J. Li, J. Xu, and H. Zeng, "Superstable transparent conductive Cu@Cu₄Ni nanowire elastomer composites against oxidation, bending, stretching, and twisting for flexible and stretchable optoelectronics," *Nano Letters*, vol. 14, no. 11, pp. 6298–6305, 2014.
- [24] S. Sorel, D. Bellet, and J. N. Coleman, "Relationship between material properties and transparent heater performance for both bulk-like and percolative nanostructured networks," *ACS Nano*, vol. 8, no. 5, pp. 4805–4814, 2014.
- [25] D. Langley, G. Giusti, C. Mayousse, C. Celle, D. Bellet, and J. P. Simonato, "Flexible transparent conductive materials based on silver nanowire networks: A review," *Nanotechnology*, vol. 24, no. 45, p. 452001, 2013.
- [26] S. Ye, A. R. Rathmell, Z. Chen, I. E. Stewart, and B. J. Wiley, "Metal nanowire networks: The next generation of transparent conductors," *Advanced Materials*, vol. 26, no. 39, pp. 6670–6687, 2014.
- [27] J. Di, S. Yao, Y. Ye, Z. Cui, J. Yu, T. Ghosh, Y. Zhu, and Z. Gu, "Stretch-triggered drug delivery from wearable elastomer films containing therapeutic depots," *ACS Nano*, vol. 9, no. 9, pp. 9407–9415, 2015.
- [28] I. S. Jin, J. Choi, and J. W. Jung, "Silver-nanowire-embedded photopolymer films for transparent film heaters with ultraflexibility, quick thermal response, and mechanical reliability," *Advanced Electronic Materials*, vol. 7, no. 2, p. 2000698, 2021.
- [29] T. Kim, Y. W. Kim, H. S. Lee, H. Kim, W. S. Yang, and K. S. Suh, "Uniformly interconnected silver-nanowire networks for transparent film heaters," *Advanced Functional Materials*, vol. 23, no. 10, pp. 1250–1255, 2013.
- [30] P. C. Hsu, S. Wang, H. Wu, V. K. Narasimhan, D. Kong, H. R. Lee, and Y. Cui, "Personal thermal management by metallic nanowire-coated textile," *Nano Letters*, vol. 15, no. 1, pp. 365–371, 2015.